SB³C2023
Summer Biomechanics, Bioengineering and Biotransport Conference
June 4-8, Vail, CO, USA

IMPACT OF WALL DISTENSIBILITY ON EMERGING FEATURES OF CAROTID BIFURCATION HEMODYNAMICS

Sara Zambon (1), Mariachiara Arminio (1), David A. Steinman (2), Claudio Chiastra (1), Umberto Morbiducci (1), Diego Gallo (1)

(1) PolitoBIOMed Lab, Department of Mechanical and Aerospace Engineering, Politecnico di Torino, Turin, Italy

(2) Biomedical Simulation Lab, Department of Mechanical & Industrial Engineering, University of Toronto, Toronto, ON, Canada

INTRODUCTION

Recent evidence suggests that near-wall as well as intravascular hemodynamics are of pivotal importance in the onset and progression of atherosclerosis at the carotid bifurcation [1,2]. In detail, helical flow has been associated with *in vivo* markers of early atherosclerosis [1], and a 5-year longitudinal study has shown that intra-cycle variability of the wall shear stress (WSS) topological skeleton (i.e., contraction/expansion action on the endothelium) is associated with intima-media thickening after carotid endarterectomy [2]. However, all those studies relied on computational fluid dynamics (CFD) modeling under the rigid wall assumption. Here, the effect of wall distensibility on these emerging features of the carotid bifurcation hemodynamics is explored by implementing fully coupled two-way fluid-structure interaction (FSI) simulations accounting for prestress of the arterial wall, anisotropic material properties, and external tissue support. Furthermore, the relationship between hemodynamic and structural quantities is explored.

METHODS

The diastolic volumetric fluid domains of five ostensibly healthy carotid bifurcations were reconstructed from contrast-enhanced magnetic resonance (MR) angiography, including at least 15 radii of the proximal common carotid artery (CCA) [1]. The carotid structural domains were generated with constant subject-specific thickness derived from edge-enhanced black blood MR images. Subject-specific volumetric flow rates were extracted from phase-contrast MR measurements [1] and prescribed as boundary condition at the CCA inflow section. A 3D-0D coupling scheme was applied at the external and internal carotid artery (ECA and ICA) outflow sections with three-element Windkessel models tuned to match subject-specific measured flow splits and age-adjusted pressure curves [3]. On each geometry, FSI and CFD simulations were carried out using Simvascular [4]. For the FSI simulations, the arbitrary Lagrangian-Eulerian formulation was used [4]. The anisotropic nonlinear Holzapfel-Gasser-Ogden model was implemented to simulate the wall mechanical properties accounting for the presence of two families of collagen fibers aligned along two directions $\hat{\mathbf{a}}$ and $\hat{\mathbf{b}}$, according to the following strain energy function:

$$\bar{\Psi} = \frac{\mu}{2}(\bar{I}_1 - 3) + \frac{k_1}{2k_2}\sum_{j=4,6}\left[e^{k_2\left[\kappa\bar{I}_1+(1-3\kappa)\bar{I}_j-1\right]^2}-1\right] \qquad (1)$$

where μ is the isotropic matrix shear modulus, $\bar{I}_1 = trace(\bar{\boldsymbol{C}})$, $\bar{I}_4 = \hat{\boldsymbol{a}} \cdot \bar{\boldsymbol{C}} \cdot \hat{\boldsymbol{a}}$ and $\bar{I}_6 = \hat{\boldsymbol{b}} \cdot \bar{\boldsymbol{C}} \cdot \hat{\boldsymbol{b}}$, with $\bar{\boldsymbol{C}}$ being the isochoric right Cauchy-Green tensor, $\hat{\boldsymbol{a}}$ and $\hat{\boldsymbol{b}}$ are the fiber orientation unit vectors obtained from the directions $\widehat{\boldsymbol{e_1}}$ and $\widehat{\boldsymbol{e_2}}$ of the principal stresses σ_1 and σ_2, k_1 and k_2 are stress-like and dimensionless nonlinearity parameters respectively, and κ accounts for the dispersion of each fiber family around its principal direction. The material parameter values proposed in [5] by fitting experimental data were adopted. The fiber orientations were determined from the initial loading state [5]. To do so, the so-called prestress tensor was iteratively obtained by balancing diastolic intraluminal blood pressure from CFD simulations until zero displacement is obtained [4], as illustrated in Fig. 1. Viscoelastic support of the tissue surrounding the carotid outer wall was accounted for by imposing a Robin-type boundary condition [4]. For the purpose of comparison, rigid wall CFD simulations were carried out with the same fluid mesh and simulation settings as in FSI simulations. Maximum edge sizes of the tetrahedral radius-based meshes were 0.17 mm (fluid domain) and 0.39 mm (solid domain).

In addition to the canonical time-average WSS (TAWSS) and oscillatory shear index (OSI), the variability of the WSS contraction/expansion action along the cardiac cycle was quantified by the topological shear variation index (TSVI) [2], defined as:

$$\mathrm{TSVI} = \left\{\frac{1}{T}\int_0^T [\mathrm{DIV}_w - \overline{\mathrm{DIV}_w}]^2 dt\right\}^{\frac{1}{2}} \qquad (2)$$

where DIV_w represents the divergence of the normalized WSS vector field [2] and T is the duration of the cardiac cycle. Data from all cases were pooled to identify the 20th percentile value of TAWSS and 80th percentile values of OSI and TSVI. These threshold values were used to obtain the burden of disturbed WSS by quantifying the relative surface area (SA) exposed to TAWSS below (OSI, TSVI above) the corresponding threshold value. Analogously, wall regions exposed to elevated structural stress and strain were obtained by calculating the 80th percentile of the cycle-average maximum principal stress (σ_1) and strain (ε_1) at the fluid-solid interface. The Similarity Index (SI, here defined as two times the SAs intersection over the SAs union) was adopted to quantify the co-localization of hemodynamic and structural quantities [1]. The intravascular flow was characterized in terms of cycle-average local normalized helicity (LNH) and helicity intensity h_2, given by the cycle- and volume-average of the norm of the internal product of velocity and vorticity [1]. The bifurcation region was delimited by sections CCA3, ICA5 and ECA2 (Fig. 1).

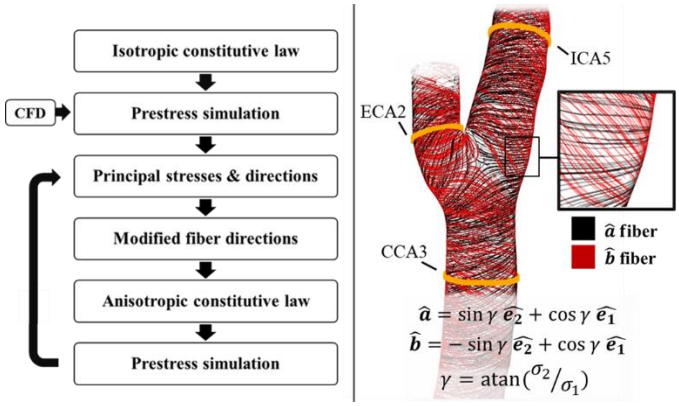

Figure 1: Prestress iterations (left panel) to determine fiber directions (right panel) and the initial loading state.

RESULTS

FSI simulations provided average values of luminal area variation at the CCA3 of 14.5%±3%, consistent with in vivo measurements [6]. TAWSS, OSI, and TSVI distributions were comparable in distensible *vs.* rigid wall simulations, both qualitatively (Fig. 2; TAWSS and OSI not shown) and quantitatively (surface-averaged TSVI values 305.1±141.0 m^{-1} *vs.* 313.1±172.4 m^{-1}, respectively). Counter-rotating helical flow patterns characterized the flow field of all models, as highlighted by LNH isosurfaces of opposite signs (Fig. 2). Rigid wall models were characterized by higher h_2 values (Fig. 2).

Maximum values of both σ_1 and ε_1 were localized at the apex of the bifurcation (Fig. 3). SI values for the couplets of hemodynamic and structural quantities are reported in Table 1. The highest co-localization was found between σ_1 and OSI or TSVI (SI=0.55, Table 1). Low SI values were found between low TAWSS and high σ_1 or ε_1 regions. SI values between high σ_1 and ε_1 regions were 0.88±0.07.

DISCUSSION

The near-wall and intravascular hemodynamic quantities investigated here were only moderately affected by wall distensibility. Thus, the rigid wall assumption seems to be acceptable when linking the considered emerging hemodynamic features and atherosclerosis initiation at the carotid bifurcation. Considering the increased complexity, cost, and inherent introduction of additional uncertainties to model wall distensibility, our findings suggest that rigid wall CFD modeling might be considered reasonable in view of a future clinical translation. With that said, the implemented FSI approach allows exploring the synergistic action between hemodynamic stresses on the endothelium and wall structural stress [7], potentially uncovering distinct or synergistic effects of these biomechanical stimuli on atherosclerosis initiation.

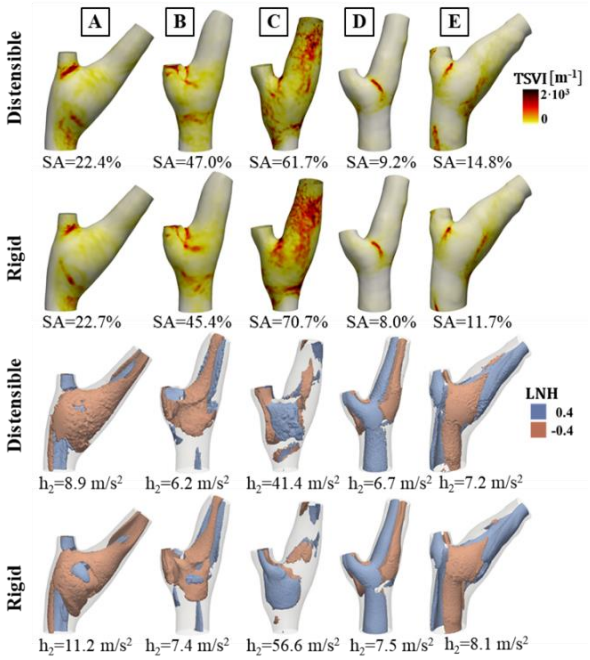

Figure 2: TSVI and LNH distributions.

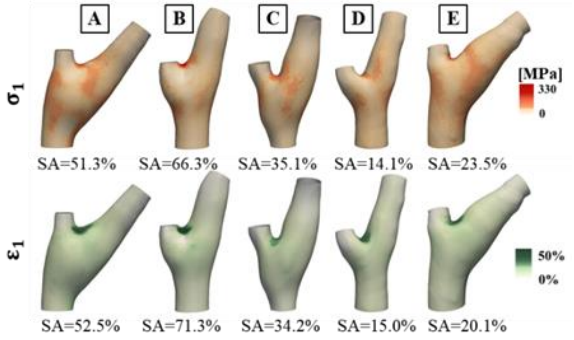

Figure 3: $\sigma_1$and ε_1 distribution at the fluid-solid interface.

Table 1: SIs between hemodynamic and structural quantities

SI (MEAN±STD)	TAWSS	OSI	TSVI
σ_1	0.12 ± 0.11	0.55 ± 0.18	0.55 ± 0.12
ε_1	0.10 ± 0.08	0.53 ± 0.18	0.55 ± 0.12

REFERENCES

[1] Gallo, D et al., *J R Soc Interface*, 15(147):20180352, 2018.
[2] Morbiducci, U et al., *Ann Biomed Eng*, 48(12):2936–2949, 2020.
[3] Hirata, K et al., *Stroke*, 37(10):2552–2556, 2006.
[4] Bäumler, K et al., *Biomech Model Mechanobiol*, 19(5):1607–28, 2020.
[5] Hariton, I et al., *J Theor Biol*, 248(3):460–470, 2007.
[6] Segers, P et al., *J Hypertens*, 42(5):638-638, 2004.
[7] Qiu, Y and Tarbell, JM, *J Vasc Res*, 37(3):147-57, 2000.